Monolithic Near Infrared Image Sensors Enabled by Quantum Dot Photodetector

Pawel E. Malinowski[1,*], Epimitheas Georgitzikis[1,2], Jorick Maes[3,4], Mehedi Mamun[1,4], Oscar Enzing[1], Fortunato Frazzica[1,5], Jan Van Olmen[1], Piet De Moor[1], Paul Heremans[1,2], Zeger Hens[3,4], and David Cheyns[1]

[1]IMEC, Kapeldreef 75, B-3001 Leuven, Belgium
[2]KU Leuven, Kasteelpark Arenberg 10, B-3001 Leuven, Belgium
[3]Physics and Chemistry of Nanostructures, Ghent University, Krijgslaan 281-S3, B-9000 Ghent, Belgium
[4]Center for Nano- and Biophotonics (NB-Photonics), Ghent University, B-9000 Ghent, Belgium
[5]Vrije Universiteit Brussel (VUB – ETRO), Pleinlaan 2, B-1050 Brussel, Belgium
[*]E-Mail: Pawel.Malinowski@imec.be, Tel.: +32 1628 1938, Fax: +32 1628 1097

Widespread deployment of infrared image sensors is prevented by high cost and low resolution. Nevertheless, narrow bandgap thin-films can enable wafer-level monolithic integration. This work describes a CMOS-compatible pixel stack based on PbS quantum dots. Inverted photodiode with a 150 nm thick absorber shows dark current of 10^{-6} A/cm^2 at -3 V reverse bias, EQE above 12% (at 1450 nm absorption peak) and 45 dB current ratio under top illumination. Optical modelling improved the top contact transparency to 70%. Additional cooling (193 K) can improve the sensitivity to 60 dB. This stack will be integrated on a CMOS ROIC, enabling order-of-magnitude infrared sensor cost reduction.

Imaging in the near infrared (NIR) wavelength range (0.7 – 1.4 μm) is essential for many applications such as low-light / night vision, surveillance, sorting or biometrics. At the same time, universal adoption of NIR sensors is compromised by higher cost and lower resolution compared to the CMOS image sensors operating in the visible range [1]. Previous reports showed the possibility of integration of thin-film photodetectors in imagers (organic [2] and quantum dots [3]) and that even with submicron pixel size [4].

In this work, we describe building blocks for realization of a monolithic infrared image sensor. We use Quantum Dot Photodetectors (QDPD) based on narrow-band PbS colloidal quantum dots [5]. These sensors can be fabricated without flip-chip hybridization of a III-V chip (Fig. 1). This has a significant effect on both cost (wafer level process feasibility, no epitaxy) and performance (resolution and pixel pitch limited only by the CMOS readout, Fig. 2). Imager spectrum can be extended from the visible range up to the wavelength of 2 μm.

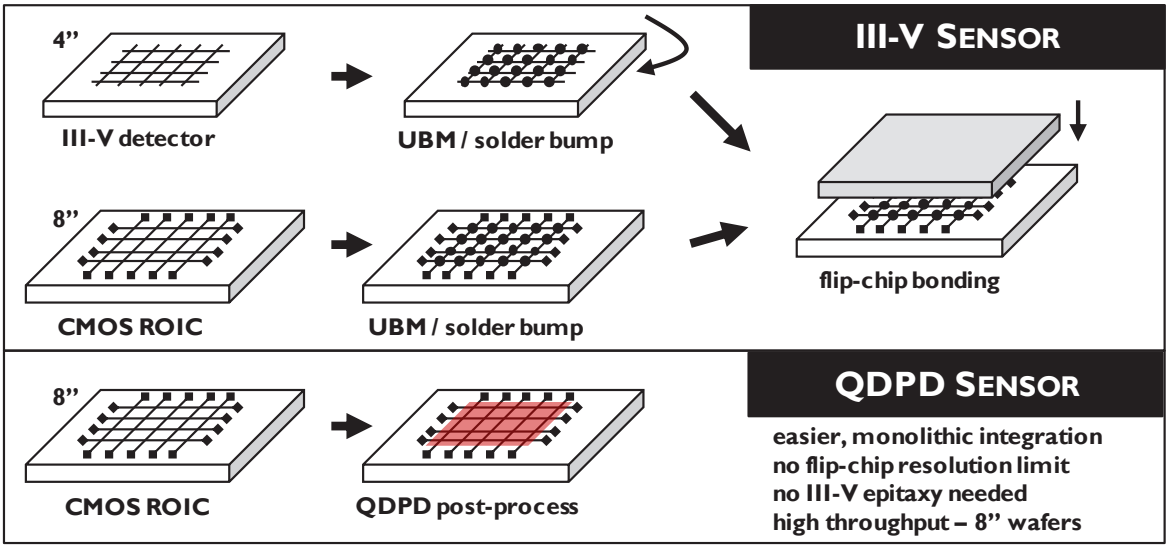

Figure 1. Integration route for a hybrid III-V infrared image sensor (top) and a monolithic quantum dot infrared image sensor (bottom).

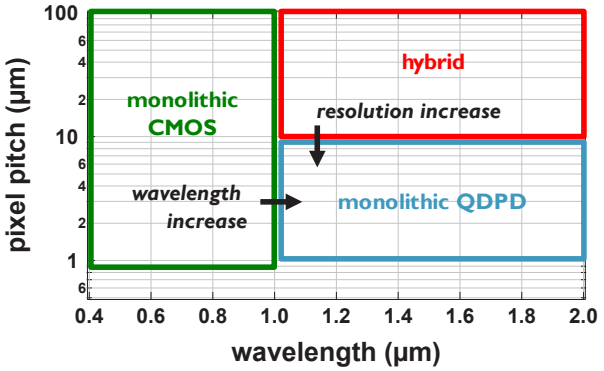

Figure 2. Positioning of a QD-based image sensor: higher wavelength than monolithic Si and higher resolution than hybrid alternatives.

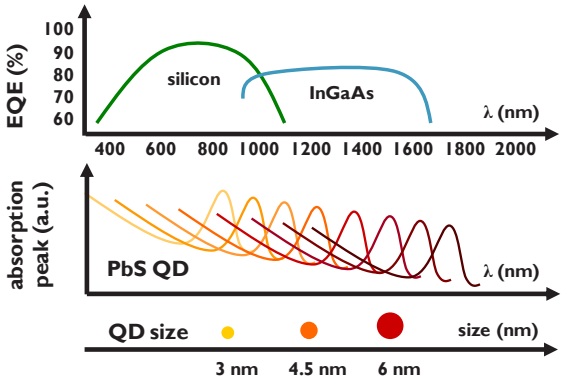

Figure 3. Absorption spectrum of quantum dots can be tuned with their size and is competitive to Si and InGaAs in the NIR range.

PbS QDs enable uncooled NIR detection up to 2 µm wavelength depending on their size (Fig. 3). In this work, the main focus is on quantum dots with 5.5 nm diameter having the absorption peak at the wavelength of 1450 nm. With smaller dots, the peak can be adjusted to add near infrared bands to the hyperspectral image sensors. With larger dots, the spectrum of InGaAs image sensors can be addressed.

To develop a photodetector stack compatible with a readout integrated circuit (ROIC) based on complementary metal-oxide-semiconductor (CMOS) technology, we use Si/SiO_2 substrates with TiN bottom contact (standard metal in the CMOS flow). A 150 nm thick, quantum dot active layer (Fig. 4) is deposited from solution as a multilayer stack. Thereon, a metal-oxide electron transport layer (ETL) is deposited to form an inverted stack, followed by the QD layers. Transmission Electron Microscope (TEM) inspection reveals perfect crystallinity within the QDs, high level of crystallinity within a single layer and random orientation between layers. On top, an organic hole transport layer (HTL) and a semi-transparent top contact are deposited.

Looking at the electrical performance (Fig. 5), single pixel test photodiodes show approximately 3 $\mu A/cm^2$ dark current density at -3 V reverse bias voltage. This value scales from pixel size of 2x2 mm^2 down to 50x50 μm^2. Photocurrent under IR light emitting diode (LED) illumination (1450 nm) through a semi-transparent top contact follows the same trend.

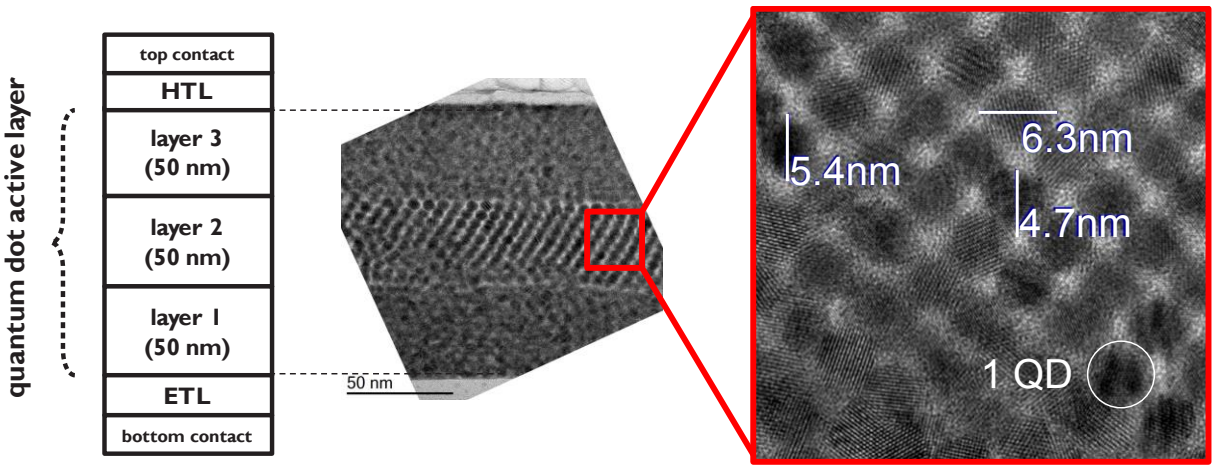

Figure 4. Cross-section (left: schematic; right: Transmission Electron Micrograph) of a 3-layer active stack based on 5.5 nm PbS quantum dots. The layers are deposited consecutively by spin-coating.

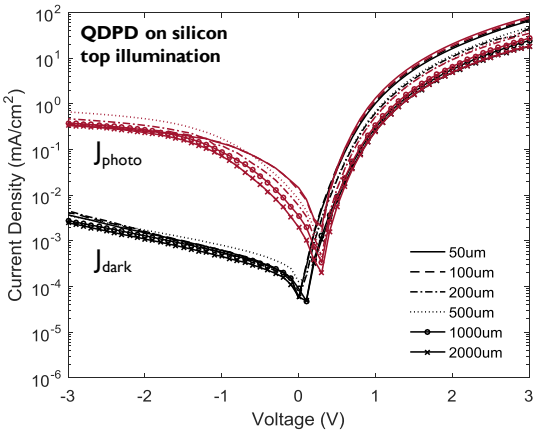

Figure 5. Dark and photocurrent density curves for different pixel sizes showing no reverse leakage scaling down to 50x50 µm^2 pixels.

In top illumination tests with IR LED and increasing irradiance, we could observe a linear increase of the photocurrent (Fig. 6). The calculated photo-to-dark current ratio is 45 dB in the reverse bias voltage range of -2 to -3 V.

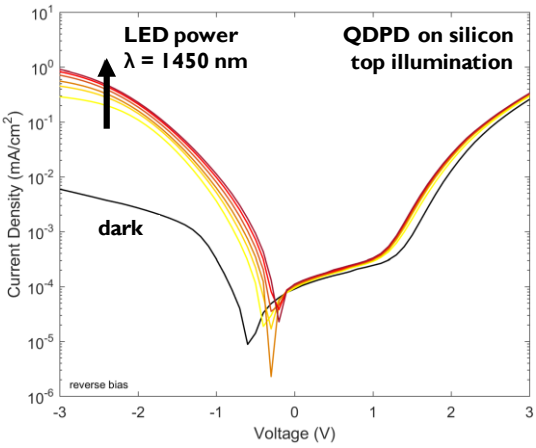

Figure 6. Current density – voltage characteristics of a QDPD on Si substrate in dark (black line) and under 1.5 µm IR LED with varying power (color lines).

External quantum efficiency (EQE) is above 12% at the absorption peak at the wavelength of 1450 nm (Fig. 7a). Even though this is still significantly lower than EQE of InGaAs photodetectors, it is at the same time unachievable by Si photodetectors. Furthermore, this absorption peak can be quite accurately tuned by the QD diameter. Fig. 7b illustrates photodetectors fabricated with three different QD sizes leading to absorption peaks at the wavelengths of 1050 nm, 1250 nm and 1450 nm. Taking the photodiode dark current as the major noise component, we can obtain specific detectivity (D*) of 1x10^{11} Jones.

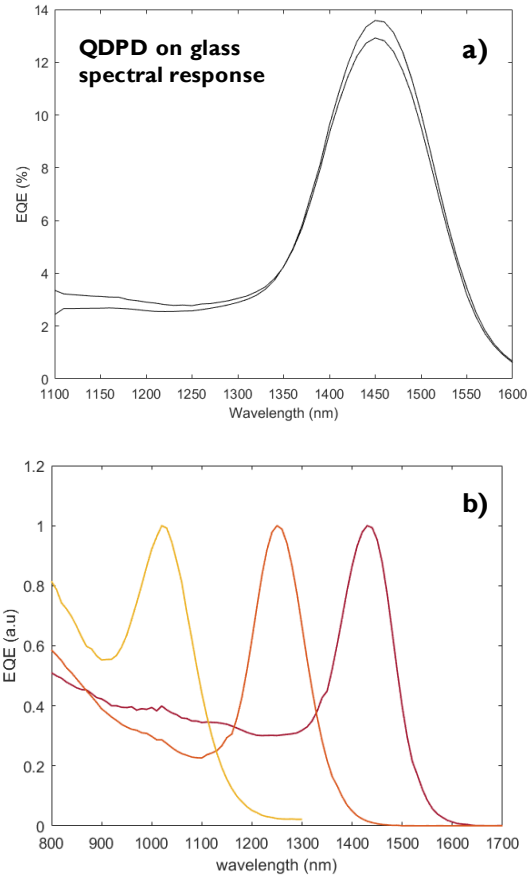

Figure 7. External Quantum Efficiency curve in the NIR wavelength range of a QDPD under -2 V reverse bias.

Standard test vehicle used for optimization of visible-range QDPDs is glass substrate with indium tin oxide (ITO) bottom contact (transparent in the visible range) and opaque top contact (for improved reflection in bottom illumination mode). In order to transfer the stacks to top-illuminated, CMOS-compatible substrate and optimize the absorption for NIR, we employ optical interference modelling with transfer matrix method. This way, we obtained experimentally verified top contact transparency of 70% in the near infrared range (Fig. 8) which is a significant boost from the standard contact structure used in the visible range. Thus, the EQE of top-illuminated photodetectors on TiN bottom contact can be further improved and reach 25%. In terms of manufacturing, the entire photodetector stack can be fabricated with standard semiconductor processing methods in the fab environment. In the final imager, the detailed optical design will strongly depend on the wavelength of interest – differing between extension of visible CIS to NIR (with same optics) and dedicated NIR imager (with infrared optics).

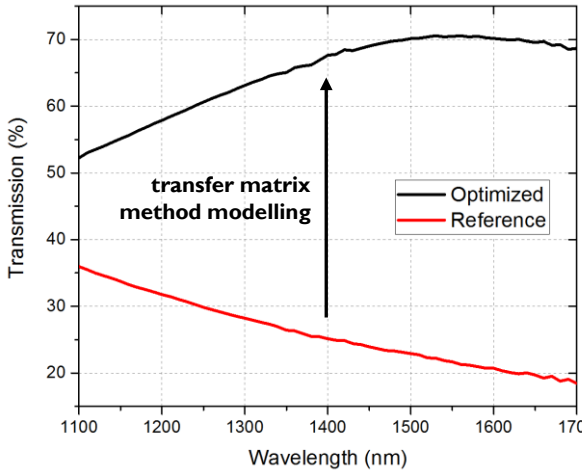

Figure 8. Top contact photodetector stack optimized for NIR transparency.

Even though PbS QDPDs enable detection at room temperature, standard IR camera packaging offers possibility of additional cooling. In our cryostat measurements, we observed that by cooling the detector to 193 K we can further improve the current ratio to over 60 dB (Fig. 9).

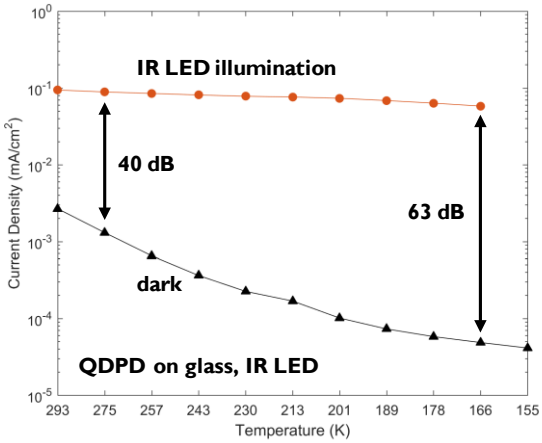

Figure 9. Dark and photocurrent vs. photodetector temperature, indicating an increasing current ratio.

In summary, the pixel stack demonstrated here shows building blocks for fabrication of a monolithic image sensor for the near infrared wavelength range. The benefits of using QDPD active stack are ease of processing, room-temperature operation, submicron active layer thickness and high EQE in NIR.

The next step of development is integration of the photodetector stack on the CMOS ROIC test chip (Fig. 10). The QDPD integration method will enable low-cost infrared cameras with resolution and pitch limited only by the ROIC design.

References

[1] P. Martyniuk, J. Antoszewski, M. Martyniuk, L. Faraone, A. Rogalski, P. Martyniuk, J. Antoszewski, M. Martyniuk, L. Faraone, and A. Rogalski, "New concepts in infrared photodetector designs," Appl. Phys. Rev., vol. 041102, no. 1, (2014).

[2] D. Baierl, L. Pancheri, M. Schmidt, D. Stoppa, G.-F. D. Betta, G. Scarpa, P. Lugli, "A hybrid CMOS-imager with a solution-processable polymer as photoactive layer," Nat. Commun., vol. 3, p. 1175 (2012).

[3] T. Rauch, M. Boberl, S. F. Tedde, J. Furst, M. V. Kovalenko, G. N. Hesser, U. Lemmer, W. Heiss, O. Hayden "Near-infrared imaging with quantum-dot-sensitized organic photodiodes," Nat. Phot., vol. 3, p. 332 (2009).

[4] M. Takase, Y. Miyake, T. Yamada, T. Tamaki, M. Murakami, Y. Inoue "First Demonstration of 0.9 µm Pixel Global Shutter Operation by Novel Charge Control in Organic Photoconductive Film," IEDM'15, p. 30.2 (2015).

[5] C. Hu, A. Gassenq, Y. Justo, K. Devloo-Casier, H. Chen, C. Detavernier, Z. Hens, and G. Roelkens, "Air-stable short-wave infrared PbS colloidal quantum dot photoconductors passivated with Al2O3 atomic layer deposition," Appl. Phys. Lett., vol. 171110, pp. 1–5 (2014).

Status Now	Next Step
■■■ EQE in near IR > 10%	QD with different size
■■□ Dark current ~1 µA/cm²	QDPD stack improvement
■■□ CMOS bottom contact	Better reflectivity
■■□ Transparent top contact	ARC* optimized for IR
■□□ Pixel size scaling down	Pixel size < 10 µm
■□□ Custom ROIC design	Test ROIC fabrication
□□□ 2D detector array	FPA integration on CMOS

ARC – Anti-Reflective Coating

Figure 10. Status of QDPD image sensor integration and the next foreseen steps.